Recent developments of the OSCAR calculational system, as applied to selected examples from IAEA research reactor benchmarks

R. H. Prinsloo[1], F. A. Van Heerden[1], D. Botes[1], R. Mudau[1]

1) South African Nuclear Energy Corporation (Pty) Ltd, P.O. Box 582, Pretoria, 0001 South Africa

Corresponding author: rian.prinsloo@necsa.co.za

Abstract. The OSCAR-4 code suite is a nodal diffusion based calculational system, which has been used over many years for research reactor support. It is primarily used to support the operation of the SAFARI-1 research reactor at Necsa, South Africa, but is also applied at various other international research reactors (such as HOR, HFR and MNR). Recently, the next generation OSCAR system (termed OSCAR-5) has been under development, with specific focus on the challenges which highly heterogeneous research reactor core designs pose – in particular with regard to core design and core-follow type analyses. The main aim of the new development is the seamless integration between high fidelity and standard core analysis methods. A detailed heterogeneous model is constructed in a code-independent front-end system, which is then capable of deploying the model to all codes connected to it. In particular, automatic input generation is available for Monte Carlo codes like MCNP and Serpent, as well as the nodal diffusion solver in OSCAR-4. The deployment to a nodal diffusion code uses advanced homogenization and nodal equivalence methods to ensure a theoretically minimized discrepancy between the heterogeneous and homogeneous solutions. The nodal model is developed in a staged process, allowing tight monitoring and control of the model error as compared to the reference heterogeneous Monte Carlo model. In particular, all non-fuel homogenized multi-group cross-sections are generated from a set of full-core heterogeneous calculations, while fuel models are generated from typical, often infinite lattice, environments. The use of infinite lattice models results in the so-called environmental error on the nodal equivalence parameters, which in the new system may be remedied via various correction schemes in the nodal diffusion solver. The numerical impact of these approaches is illustrated on the SAFARI-1, OPAL and IPEN reactor benchmarks as they appear in the ongoing IAEA CRP T12029 on multi-cycle depletion and activation analysis.

1. Introduction

Reactor physics codes used in aid of reactor operational support generally adopt either a deterministic or stochastic methodology. The deterministic codes have historically been the primary workhorse for cycle follow, and fuel management type analysis, while stochastic codes (i.e. Monte Carlo) have been used to construct high fidelity models for snap-shot analysis. This strict separation has become less pronounced with recent advances in computing power. Hand-in-hand with these developments, the verification and validation burden on reactor analysts in the research reactor support space has grown significantly, especially as the designs of modern research reactors have increased in power level and complexity of fuel designs.

With these two trends in mind, it has become increasingly important to allow the use of high fidelity, fit-for-purpose analysis tools applied in synergy, but simultaneously ensure that consistency is retained between code models in this multi-code environment.

The OSCAR-4 code suite, developed at Necsa, South Africa, is a nodal diffusion based calculational system, which has been used over many years for research reactor analyses [1]. It is primarily used to support the operation of the SAFARI-1 research reactor at Necsa, South Africa, but is also applied at various other international research reactors, such as HOR (TU-

Delft, The Netherlands), HFR (NRG, The Netherlands) and MNR (McMaster University, Canada) as a reactor core-follow and core reload design tool.

In this work, the next generation OSCAR system (termed OSCAR-5) is described in response to this changing and challenging research reactor analysis environment. The various capabilities of the new system are demonstrated on a sub-set of full-core depletion benchmarks as specified in the ongoing IAEA CRP T12029 on multi-cycle depletion and activation analysis [2]. In particular, models are developed in the system and results compared to experimental data for:

- depletion of a fissile rig in the ex-core region of the IPEN reactor in Brazil, with associated Gold foil activation experiments;
- 15 operating cycles of the SAFARI-1 reactor in South Africa with focus on multi-cycle reactivity and control rod calibration experiments for five cycles; and
- 5 operating cycles for the OPAL reactor in Australia (first seven cores) with focus on multi-cycle reactivity.

These three full-core experimental benchmarks are selected as a vehicle to illustrate the varying challenges faced in supporting modern research reactor operations, and how a high-fidelity, multi-code analysis approach as employed in OSCAR-5 could prove useful.

2. The OSCAR-5 system

2.1. Overview

The OSCAR-5 system aims to allow for multi-code, multi-physics support for research reactor analysis, with the primary aim to allow the use of fit-for-purpose tools in support of reactor operations. This implies finding a balance between the nature of a specific calculational application and the level of detail and fidelity utilized in achieving the result.

The OSCAR-5 system incorporates a powerful pre- and post-processing system, which maintains a consistent model, and manages the passing of data between target codes. FIG. *1* gives a schematic outline of the system.

The main entry point to the system is the construction of a unified, code-independent system model. A detailed model of each assembly type as well as the reactor pool (or reflector) is built using the Constructive Solid Geometry (CSG) module of the system. Assembly models are combined in an assembly library, from which full-core configurations are constructed. All material properties (isotopic composition and nominal material state, etc.) are also defined in a code-independent fashion.

The model building process is facilitated in the system via extensive visualization schemes, allowing 3D rendering with multiple filters to isolate the components and materials being considered. This can be done at both component and core level. Macros for the automatic creation of typical component types (e.g. plate type fuel assemblies), geometry processing and mesh optimization schemes as well as mesh completion algorithms all assist in the creation and final deployment of the model.

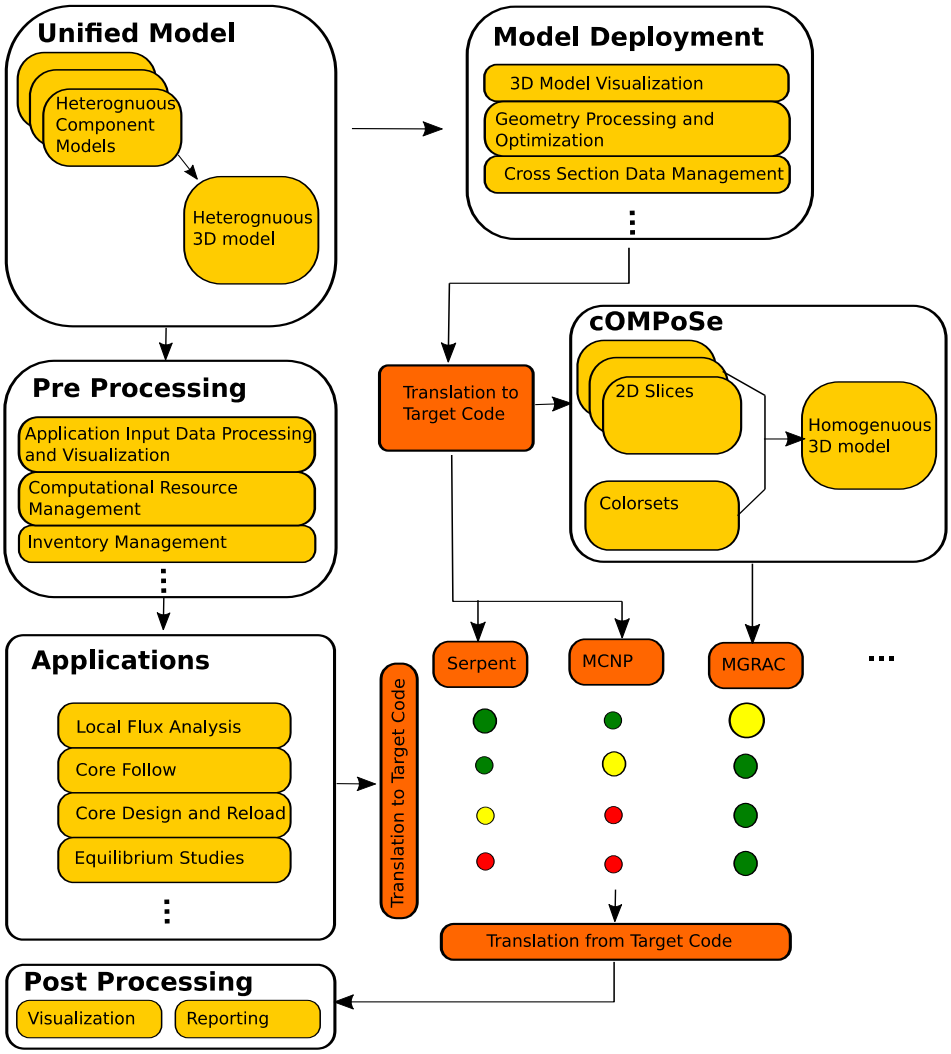

FIG. 1. OSCAR-5 system design.

Translators are used to write the geometry and material description of the model to the input for target codes that use detailed geometry. These translators are defined once in the system, and therefore do not depend on the model. This mechanism also ensures that the model remains consistent when it is exported to multiple codes.

Detailed assembly and core models cannot be used directly in a nodal diffusion solver, since it requires an additional homogenization. The cOMPoSe (OSCAR Model Preparation System) tool is used to systematically move from the heterogeneous unified description with point wise cross section data, to a set of homogenized mixtures with energy condensed to a few group representation.

Once a suitable model is prepared, it can be deployed to various analysis applications. The system also treats the input and execution of applications in a code-independent manner. In particular, all input data is provided through a unified system interface, with facilities to visualize and further manipulate the data. Moreover, the deployment to various hardware

architectures, ranging from single node workstations, to multi-core, multi-node computing clusters, are automated and handled internally. This allows one to match the best available hardware to the intended target code. A generic inventory management system, which stores the material states of burnable assemblies, makes it possible to use analysis codes lacking this feature for long term core management. It also allows the transfer of assembly states, using a number of options to merge and expand isotopic compositions, to the different codes connected to the system, so that calculations can be performed at any time or state point by the most appropriate tool.

FIG. *1* shows the neutronic codes currently coupled to the system, where the dot under each code illustrates the suitability of that code to the intended application. A green dot means the code is perfectly suitable, a yellow dot means it can be used but is not necessarily the best choice, and a red dot indicates that, although possible, the code is not well suited due to feature or resource limitations. The size of the dot indicates the error or level of uncertainty associated with each code for that application. For instance, although the nodal diffusion solver MGRAC can be used to estimate local flux values in the system, the associated error would be large. The Monte Carlo codes Serpent or MCNP would be much better choices, with MCNP more favourable since it incorporates better estimators in its detector response models. On the other hand, for equilibrium studies where a final core mass distribution is the main outcome, MGRAC will give fairly accurate results in a reasonable amount of computing time, while the Monte Carlo codes will consume many thousands of CPU hours.

This multiplicity naturally allows for the development of verification and validation schemes, since the main benefit and goal of the system is that, no matter what code is used, the model and input data remain consistent.

2.2. cOMPoSe

For the sake of very fast calculation of the neutron flux distribution, one may need to move from a full detail, heterogeneous model utilizing transport theory for neutronic analysis, to a coarse (or nodal) homogenized representation suitable for diffusion theory. The homogenized model would contain a limited number of large nodal (assembly size) meshes and must be prepared in such a way that it captures as much of the neutronic behaviour of the heterogeneous model as possible, a constraint that requires many factors to be taken into consideration. In the cOMPoSE system, this typically involves the following steps:

1. For a given core configuration, a coarse radial mesh is chosen, which defines the node sizes. This is typically done in such a way that the fuel pitch is preserved, so that fuelled assemblies fill one node. Next, a number of axial slices are chosen along the length of the model, with each slice capturing important features of the model, while attempting to limit the amount of axial heterogeneity within a slice. This effectively divides the model into a number of two-dimensional layers.

2. Homogenized cross sections are then calculated on the nodal mesh for each axial layer, by performing a two-dimensional transport calculation over the entire slice. Generalized equivalence theory is used to ensure that reaction rates and leakages are preserved for each node.

3. Fuelled assemblies, or any other assembly that either undergoes state changes (e.g. burnup), or does not stay in a fixed position in the core, needs additional treatment. This is because, for a fast operational support tool, we do not want to re-homogenize the entire core every time the configuration changes. Thus, fuelled and other loadable assemblies are treated in a more traditional fashion, by performing assembly level lattice calculations in approximate environments (so-called colorsets). These calculations also account for burnup and state changes. It is important to note that, since it is difficult to capture all the environments a loadable assembly would experience, this is a major source of error, and its effect must be carefully monitored.

4. Finally, all two-dimensional layers are stacked together to form a three-dimensional model. Since axial leakage is not preserved, this is another potential source of error.

During each step of the process, the system gives feedback on the errors (as compared to the detailed heterogeneous model) incurred. Since the errors at the stages of 2D cut generation, lattice replacement and 3D construction are now more traceable, they can be refined, so that one ends up with a nodal diffusion model with acceptable and well-quantified error margins.

In this work Serpent is used to homogenize the two-dimensional slices, while the homogenization of fuelled or loadable components is performed by the HEADE code (in-house lattice code). HEADE uses collision probability methods to generate few-group assembly homogenized equivalence parameters. As a final output a single run-time cross-section library is produced, which is used along with the final homogenized three-dimensional model, suitable for use in the nodal diffusion solver MGRAC.

2.3. MGRAC

In MGRAC, the calculation of the steady-state neutron flux distribution is based on the solution of the three-dimensional, multi-group, time-independent diffusion equation by means of a modern transverse-integration nodal method [3]. MGRAC utilizes a microscopic depletion model. Given the nodal approach utilized in MGRAC, it is capable of performing a full cycle depletion calculation on a standard desktop machine in a few minutes.

2.4. Serpent

Serpent, a Monte Carlo criticality and burnup code developed at the VTT Technical Research Centre of Finland [4], is capable of cell-level and full-core calculations for determining group

constants as well as performing as a standalone simulation suite. Serpent's main advantage is the use of a fast tracking algorithm, significantly increasing performance in complicated geometries, and the use of a unified energy mesh to accelerate cross section queries.

2.5. MCNP6

MCNP6 is a well-known general purpose Monte Carlo code for the transport of neutral (and selected charged) particles. The code has advance tally features, making it the preferred tool for difficult, localized flux estimation. Material activation and burnup features were introduced in version 6 [5].

3. Benchmarks and results

The IAEA CRP T12029 [2] is an effort to collate multi-cycle depletion and material activation benchmarks to support calculational code verification and validation. In this paper, a subset of these benchmarks is used to demonstrate some of the features in the OSCAR-5 system. The intent is to not fully discuss the benchmark specification and related experimental data (this will be published by the IAEA in due course), but rather to use the benchmarks to highlight particular challenges typically faced by analysts in the process of research reactor calculational support. In particular, the following issues are highlighted for each of the benchmarks:

1. In the IPEN benchmark, the benefit of utilizing multiple Monte Carlo codes (MCNP6, Serpent), deployed from a single unified heterogeneous reactor model, is demonstrated.
2. In the SAFARI-1 benchmark, the cOMPoSe sub-system is utilized to deploy a MGRAC nodal core model alongside a full-core Serpent model for multi-cycle depletion modelling. The nodal model is developed with associated error estimation, which is shown to predict the accuracy of the eventual experimental comparisons.
3. In the OPAL benchmark model, the same approach is applied as for SAFARI-1 for multi-cycle depletion, but this time with a series of necessary adaptations for modelling such a high leakage, heavy water reflected core with burnable poisons. In particular, the capability of the unified model to define various burnup zone sizes in both the Monte Carlo and homogenized models is demonstrated.

3.1. IPEN benchmark

Benchmark description

The IPEN/MB-01 reactor [6] consists of a 28×26 square array of fuel pins immersed in an open top, cylindrical moderator tank. For the experiments, a reflector box filled with heavy water was present on the west side of the fuel pin array. All irradiation targets were placed within a central column passing through the heavy water box. This central column is open to the pool, and is therefore filled with light water.

In the Molybdenum experiment, ten 19.58% enriched UAl-Al target plates were irradiated. The plates were placed in two target holders, and inserted into the central column of the heavy water reflector box. Irradiation time was 1 hour, with the reactor power at 108 W. The

induced Mo-99 activity was determined through the measurement of both Mo-99 and mTc-99 gamma peaks. For this experiment, our model only attempts to reproduce the final Mo-99 activity estimate.

For the gold foil activation experiment, five diluted gold foils were attached to a dummy (no uranium content) target plate, which was inserted into an empty target holder and placed into the central column of the heavy water reflector box. Irradiation time was 1 hour with the reactor power at 108 W. Resulting radiative capture rates were estimated using gamma spectroscopy.

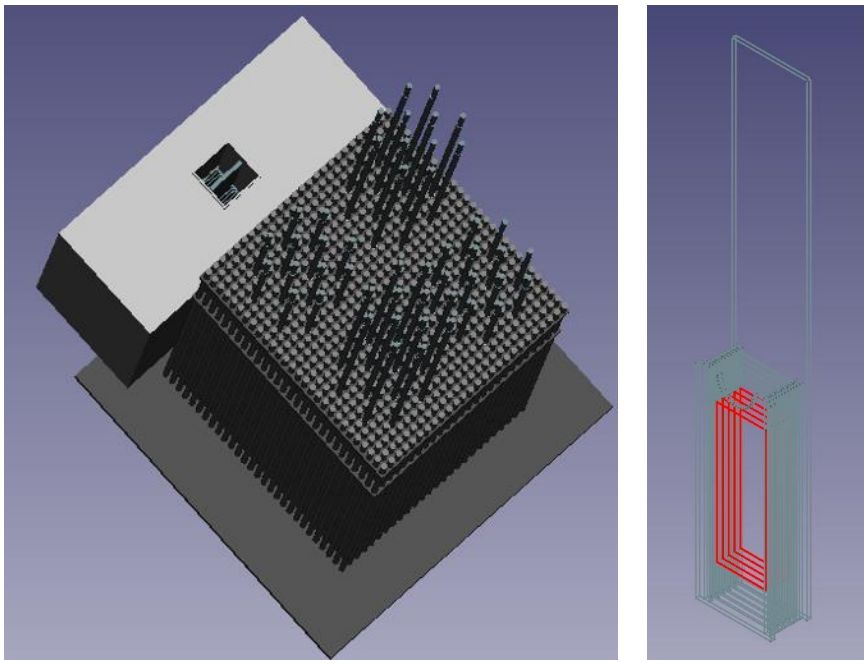

FIG. 2. 3D view of IPEN OSCAR-5 unified model (left) and target holder with target plates (right).

Model, results and discussion

The two experiments performed at the IPEN/MB-01 reactor were modelled using the OSCAR-5 system. FIG. *2* shows the unified reactor and target holder models, which were exported to the Monte Carlo codes Serpent and MCNP for neutronics (activation) analysis. Results obtained for the molybdenum experiment are compared to both the experimental measurements and the benchmark provider's results in FIG. *3*. Both codes performed well in this case, showing good agreement with experimental measurements. From a practical point of view, it should be noted that the Serpent calculation was significantly faster than the MCNP6 calculation, making it more appropriate for routine calculations of this nature.

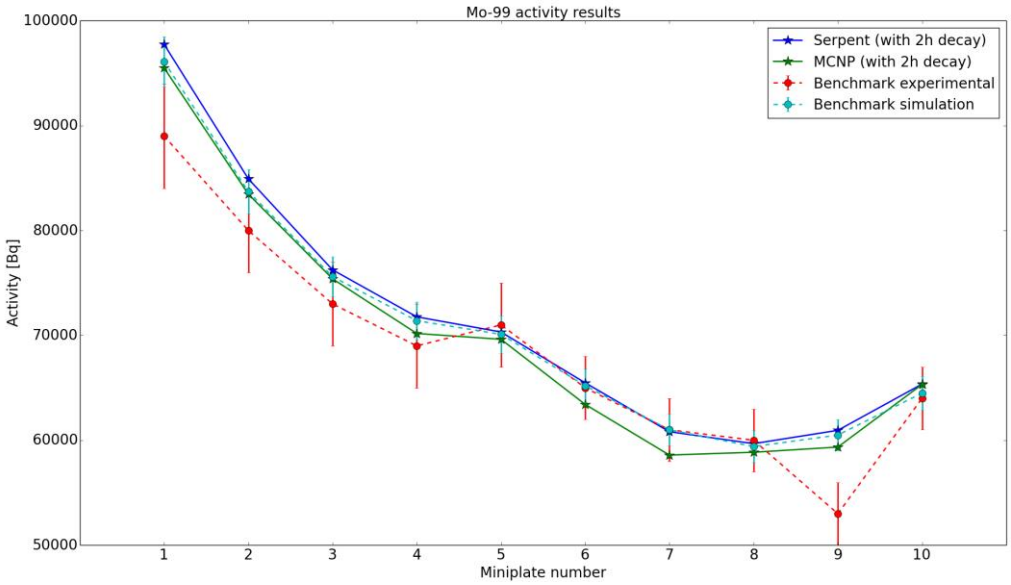

FIG. 3. Target plate depletion experimental comparison.

We now proceed to the calculation of activities in the gold foils. Calculated reaction rates are compared with the experimental values in FIG. *4*. For the calculations, only statistical uncertainties are shown.

All calculated results consistently under-predict the measured reaction rates. Statistical uncertainties are quite high, suggesting that significantly more histories should be simulated, or variance reduction techniques should be applied. The weakness of the collision density estimator in Serpent is particularly apparent here, as 10 times more histories were simulated in Serpent compared to MCNP6, but the errors remain more than twice as high.

These two experiments show how the deployment of the unified model to both MNCP6 and Serpent allows for each code to be used according to its design strengths, and in the process better support verification and validation of the developed models.

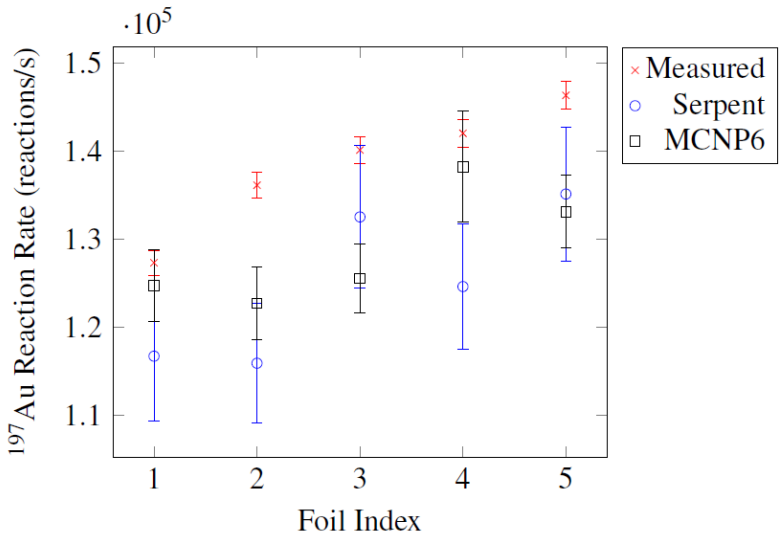

FIG. 4. Gold foil activation experimental comparison.

3.2. SAFARI-1 benchmark results

Benchmark description

SAFARI-1 is 20MW tank-in-pool type MTR utilized primarily for isotope production. The core is light-water moderator and cooled, and beryllium reflected. There are 26 fuel elements (19.75% enriched) and six follower type control rods.

Two of the benchmark experiments are analysed here. Experiment 1 refers to the multi-cycle reactivity estimation of the operational period from C1108-1 to C1211-1 (15 cycles of approximately 30 days each).

Experiment two refers to control rod calibration experiments. In each cycle for which fresh control elements are loaded, control rod calibration experiments are performed at BOC. This occurs at cycles C1201-1, C1204-1, C1208-1 and C1211-1.

Model, results and discussion

The OSCAR-5 system is used to prepare a detailed, code independent model for the SAFARI-1 benchmark problem which is shown in FIG. *5*.

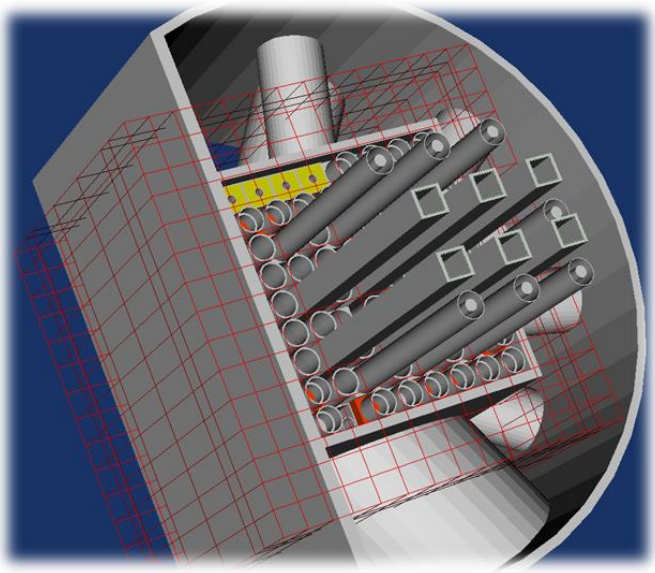

FIG. 5. 3D view of SAFARI-1 OSCAR-5 unified model.

The overlay mesh on FIG. 5 indicates the choice of homogenized zones (or nodalization scheme). This heterogeneous model is exported to Serpent to perform criticality and burnup analysis. The model is also used to generate a set of homogenized cross-sections condensed to six energy groups on the associated nodal mesh for the deterministic nodal solver MGRAC.

As discussed in Section 2.2, the nodal model is developed in a staged process, allowing control of the model error as compared to the reference heterogeneous Serpent model. In particular, all non-fuel homogenized multi-group cross-sections are generated from a set of 2D full-core heterogeneous calculations, while fuel models are generated from an infinite

lattice environment. Table I shows the staged results of the model building process and the errors introduced at each step. In particular the All Rods Out (ARO) and All Rods In (ARI) cuts are analyzed here, although the final nodal model is constructed from six cuts.

TABLE I: Error control during model building process.

Model description	**k-eff**	**Max ass. power error (%)**
Serpent 2D ARO	1.33530	-
MGRAC 2D ARO	15 pcm error	0.63
MGRAC 2D ARO-infinite fuel	300 pcm error	5.23
Serpent 2D ARI	1.05232	-
MGRAC 2D ARI	180 pcm error	0.80
MGRAC 2D ARI-infinite fuel	690 pcm error	8.02
Serpent 3D rods mid core	1.09924 (± 0.00017)	-
MGRAC 3D rods mid-core	380 pcm error	4.25

The use of this approximate environment in generating fuel cross-sections introduces an environmental error in the nodal equivalence parameters, which can be seen when going from a "MGRAC 2D" calculation to a "MGRAC 2D-infinite fuel" calculation. This error is the largest for the all rods in (ARI) case because the fuel next to control rods sees a very different core environment than the fuel next to fuel (infinite fuel environment). The ARO case has a maximum fuel element power error of 5.2 % and an average error of 1.8%.

Analyzing the spatial distribution of these errors, we observe that the errors are primarily distributed around the control rod follower positions, which all exhibit a negative error. The immediately surrounding fuel clearly does not see an infinite lattice environment either, and shows larger errors. If required, more advanced choices for colorset fuel models could be employed to remedy these errors further. Finally, the step in going from a MGRAC 2D model to a MGRAC 3D model also introduces a small additional error in the final homogenized representation of the core.

The reactor will typically operate with the control rods somewhere between mid-core and all rods out (ARO), so one can expect the MGRAC model to be within roughly 380 pcm from reference and with a maximum assembly power error of 4.25 %.

We perform the multi-cycle depletion with both deployed MGRAC and Serpent models, and compare the behaviour in FIG 6. We note quite consistent behaviour between the two models. A number of clear outliers are visible, which typically occur during start-up, shutdown, and scram events. After filtering out the outliers, the average value and standard deviation of the multi-cycle k-eff yields 1.00508 and 537 pcm respectively for OSCAR-5/Serpent whereas the corresponding values for OSCAR-5/MGRAC are 1.00329 and 417 pcm. This confirms the model building prediction of the accuracy of the OSCAR-5/MGRAC as compared to the OSCAR-5/Serpent model to be within 380 pcm, as expected based on the results in Table I.

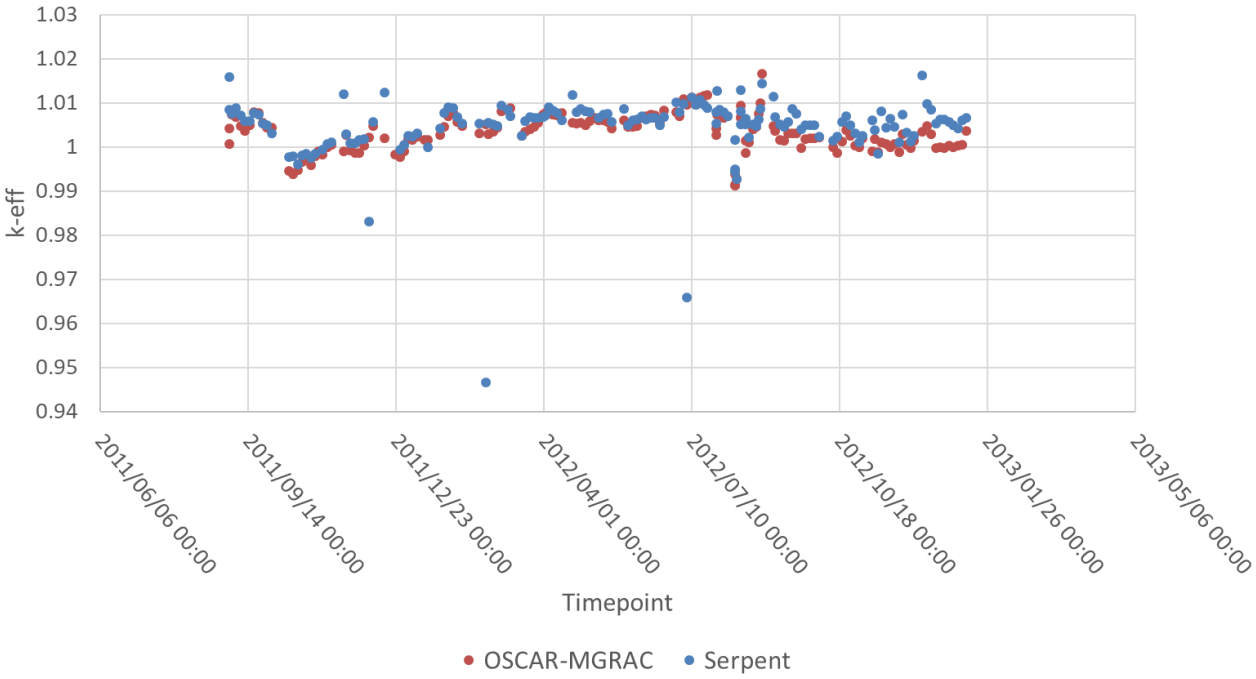

FIG. 6. OSCAR-5 multi-cycle reactivity estimate.

The relatively large standard deviation exhibited by both codes may be related to two distinct approximations that are present. Firstly, commercially sensitive rig structures were replaced with homogeneous representations, and secondly, no rig loading and unloading schedule was provided. Given the nature of SAFARI-1 operations, the loading of in-core rigs could easily account for this level of "noise" in reactivity estimates.

We move on to Experiment 2. Detailed control rod calibration curves have been calculated for each rod in every cycle where calibration experiments were conducted in. Of interest in this paper is the total worth error per position, as analyzed over the set of provided cycles, from both OSCAR-5/MGRAC and OSCAR-5/Serpent models.

The error in total worth estimate per rod, as tabulated over all the cycles in which the control rod calibration experiment was conducted, shows good agreement between OSCAR-5/MGRAC and OSCAR-5/Serpent. Statistically the two models show similar error trends, with the OSCAR-5/Serpent model exhibiting an average error of 40 cents and a standard deviation of 29 cents. The OSCAR-5/MGRAC model shows an average value of 35 cents and a standard deviation of 26 cents.

3.3. OPAL benchmark results

Benchmark description

The OPAL reactor is a 20MW(th) open-pool type research reactor [7]. This multi-purpose reactor contains facilities for the production of medical isotopes, bulk irradiation of silicon ingots and material irradiation and activation, as well as 5 beam tubes for cold and thermal neutrons. It has a compact core, consisting of 16 (4×4) plate-type fuel assemblies and 5 control rods, and is light-water cooled. Some fuel elements contain cadmium burnable absorber wires along a portion of their active height. Surrounding the core is a heavy water

reflector vessel populated with the neutron beam tubes, irradiation facilities and a cold neutron source (CNS).

The experiment considered in this analysis is the multi-cycle depletion of the first seven operational cycles of the reactor after commissioning. Averaged plant data information is provided with the benchmark, with data aggregated on steps in the order of days.

Model, results and discussion

For this benchmark, the OSCAR-5 system is used to prepare a detailed model for the OPAL benchmark problem (shown in FIG 7). As before, we show the model with nodalized mesh already super-imposed on the unified model.

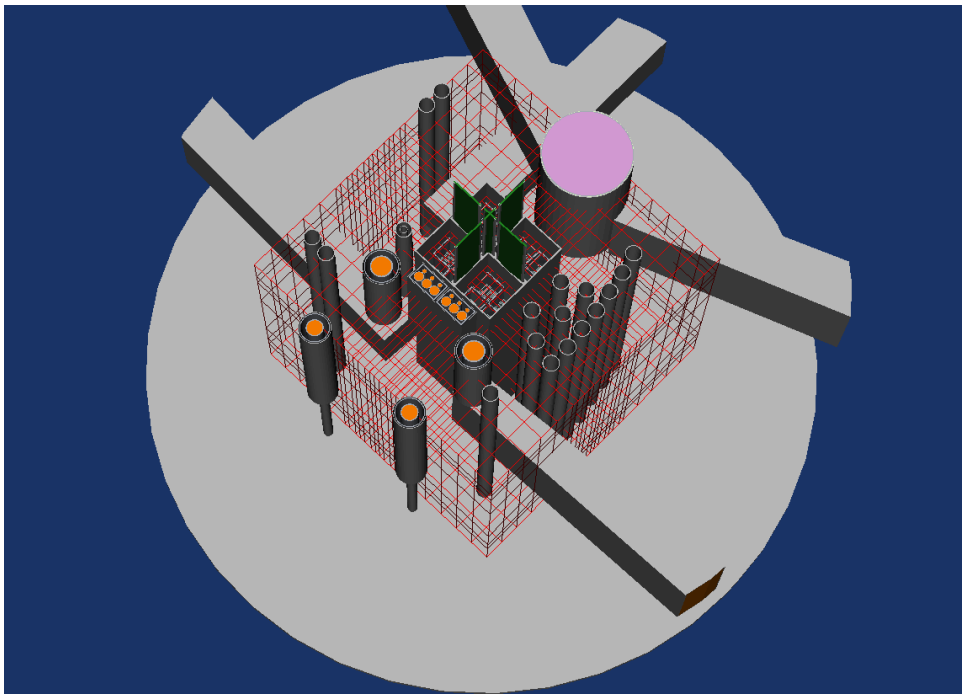

FIG. 7. OSCAR-5 3D view of the OPAL unified model.

We will progress with the model building via six full core cuts, and analyze three of them in particular: the unrodded, unwired cut (ARO-UNW), the unrodded, wired cut (ARO-W) and the rodded, wired cut (ARI-W). For these cuts, we explore the 2D errors associated with the cross-section generation process and the infinite lattice replacement step. We then evaluate two correction schemes to improve the model. The first is a special homogenization scheme for the burnable poisons, namely the usage of assembly side-fluxes based averaged cross-sections, as opposed to node-averaged flux (termed BA treatment). The second is to replace the standard nodal core representation with a sub-divided representation of 3×3 subzones for each fuel element. This is done for two reasons: improved subzone burnup and improved separation of control rods per nodal mesh for more accurate movement of rods. The model building error prediction is overviewed in Table II.

This environmental error in the nodal equivalence parameters can be seen when going from a “MGRAC 2D” calculation to a “Infinite lattice fuel”. This error is larger for cases that contain wires when no BA treatment is used, because their effect on the flux shape and spectrum is

highly localized. The use of the BA treatment does, however, mitigate this effect to a large degree for reactivity.

TABLE II: Error control during model building process

Model description	**k-eff**	**k-eff error (pcm)**	**Ass. power error Ave (Max) (%)**	**Subdivided k-eff**
Serpent 2D ARO – UNW	1.23959			
MGRAC 2DARO – UNW	1.23991	32	0.07 (0.17)	1.23979
Infinite lattice fuel	1.24739	780	0.68 (1.41)	1.24818
Serpent 2D ARO-W	1.17014			
MGRAC 2D ARO-W	1.17027	13	0.06 (0.15)	1.17025
Infinite lattice fuel	1.19462	2448	1.29 (2.7)	1.18765
BA treatment	1.16232	-782	1.16 (2.7)	
Serpent 2D ARI–W	0.94345			
MGRAC 2D ARI–W	0.94370	15	0.07 (0.15)	
Infinite lattice fuel	0.95964	1619	2.9 (4.8)	
BA treatment	0.94160	-185	2.0 (4.8)	
Serpent 3D rods mid core	1.00802			
MGRAC 3D rods mid-core	1.00499	-303	1.98 (4.1)	

The nodalized model applies a subdivided meshing scheme in the fuel elements. Fuel assemblies are subdivided into a 3×3 representation. One can observe from Table 1 that the effect of this subdivision is negligible on unwired cuts, but shows a marked improvement for the wired cuts, as the local spectrum is better captured, even without the BA treatment option.

The final 3D MGRAC model used nodal rehomogenization, the effect of which is not quantified here, but which does improve the k-eff offset from Serpent. It also used the subdivided fuel model, from an infinite lattice environment, in combination with the BA treatment. All of these combine to the 303 pcm difference from Serpent with rods at mid-core. Since the reactor will typically operate with control rods somewhere between mid-core and all rods out (ARO), we can expect the MGRAC model to be within roughly 300 to 500 pcm from reference, and with a maximum error of 3% - 4% in assembly averaged power.

We now consider the difference in behaviour in reactivity between Serpent and MGRAC over five operating cycles (C007 to C011) as shown in FIG. ***8***. Note that both these models apply the 3×3 segmented fuel representation for depletion tracking. We can quantify the differences from two perspectives, namely in-cycle behaviour and multi-cycle trend. In cycle C007, the two models differ, on average, by approximately 400 pcm (outliers removed). This cycle is particularly challenging, given that 9 assemblies contain Cd-wires, and as such the first cycle shows worse agreement in in-cycle shape that the latter cycles.

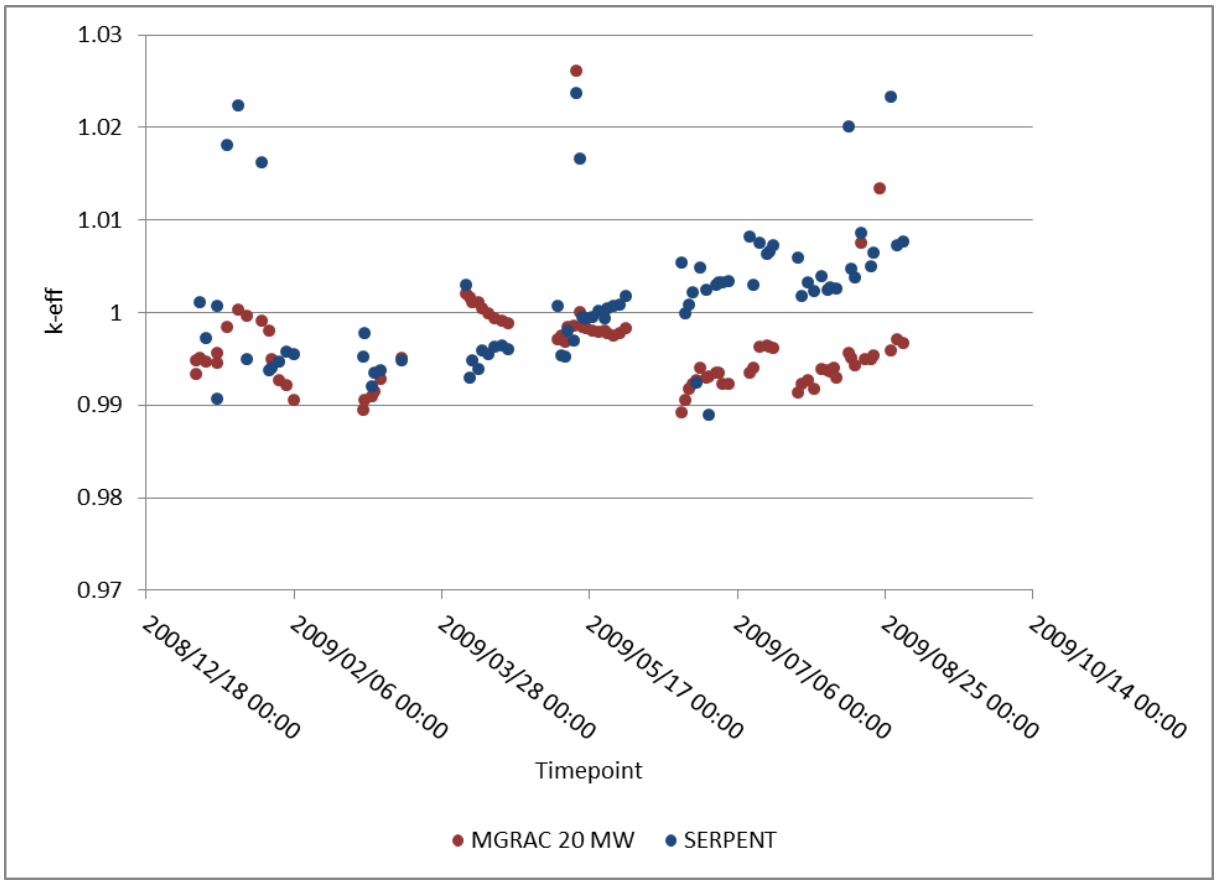

FIG. 8. OSCAR-5 reactivity estimates calculated over 7 OPAL cycles – Serpent in red and MGRAC in blue.

Secondly, we note a general upward trend in reactivity in the Serpent model, as has also been reported by the data provider in their analysis. The MGRAC model in actual fact shows the same trend, but is visually obscured by a 900 pcm drop in reactivity at the start of cycle C010. This drop still has to be further investigated, but could originate from a number of potential sources. The heavy water purity level did change significantly at the start of that cycle and the core configuration is notably different to cycle C007 with regard to fuel and Cd-wire distribution. These issues would require a regeneration of the homogenized cross-section library as well as a re-evaluation of the infinite lattice approximation error. This work remains to be done.

5. Conclusions

The advantages of using a consistent, code independent, unified reactor model which can be exported to different codes in a consistent manner depending on the intended application was demonstrated for three different examples. The OSCAR-5 system presented here allows a detailed reactor model to be maintained centrally, along with the material and history data. This represents a more complete data set that can be maintained by any single analysis tool.

The extensive capabilities of the system for moving between detailed and more approximate models through cOMPoSE allows quantification and tight control of errors introduced in the process, simplifying the verification and validation of these models. It is important to be able to distinguish between model deviations driven by provided specification as opposed to

modelling approximations. The OPAL case provides a good example hereof, since the upward trend seems to be a model independent anomaly, while the reactivity drop at cycle C010 in clearly a particular shortcoming of the homogenized approach.

Considering the three benchmarks presented in this work, it becomes possible to define in greater detail the typical errors associated with applying a given modelling approach to a particular application. In this way such multi-code, multi-benchmark activities contributes to the definition of calculational margins as needed for regulatory compliance.

6. References

[1] STANDER, G., et al., "OSCAR-4 Code System Application to the SAFARI-1 Reactor", International Conference on Reactor Physics, Nuclear Power: A Sustainable Resource, Interlaken, Switzerland (2008).

[2] INTERNATIONAL ATOMIC ENERGY AGENCY, "Benchmarks of Computational Tools against Experimental Data on Fuel Burnup and Material Activation for Utilization, Operation and Safety Analysis of Research Reactors", IAEA CRP T12029, Vienna (2015).

[3] VOGEL, D. L., WEISS, Z. J., "A General, Multigroup Formulation of the Analytic Nodal Method", International Topical Meeting on Advances in Reactor Physics, Charleston, South Carolina, USA (1992).

[4] LEPPÄNEN, J., "The Serpent Monte Carlo code: Status, development and applications in 2013", Ann. Nucl. Energy **82** (2015) 142–150.

[5] FENSIN, M., et al., "The New MCNP6 Depletion Capability". Technical Report LA–UR–12–22314, LANL (2012).

[6] DOS SANTOS, A., et al., "LEU-COMP-THERM-077 – Critical Loading Configuration of the IPEN/MB-01 Reactor", International Handbook of Evaluated Criticality Safety Benchmark Experiments, Paris, Nuclear Energy Agency (2004).

[7] INTERNATIONAL ATOMIC ENERGY AGENCY, "Research Reactor Benchmarking Database: Facility Specification and Experimental Data", Technical Reports Series No. 480, IAEA, Vienna (2015) (CD-ROM).